Int J Clin Exp Pathol 2026;19(4):168-183
www.ijcep.com /ISSN:1936-2625/IJCEP0169180

Original Article

LncRNA FENDRR is involved in the progression and cisplatin resistance of non-small cell lung cancer via binding to DGCR8

Yuan-Jin Wang[1,2*], Xiang-Ming Liu[1,3*], Shu-Yuan Li[1,3*], Meng-Wei Lv[2], Qiao Wang[2], Hao Zhang[1,3]

[1]Department of Thoracic Surgery, Affiliated Hospital of Xuzhou Medical University, Xuzhou, Jiangsu, China; [2]Department of Thoracic Surgery, Xuzhou Cancer Hospital, Xuzhou, Jiangsu, China; [3]Thoracic Surgery Laboratory, Xuzhou Medical University, Xuzhou, Jiangsu, China. [*]Equal contributors.

Received October 8, 2025; Accepted February 6, 2026; Epub April 15, 2026; Published April 30, 2026

Abstract: Objectives: Overcoming chemoresistance is a major therapeutic challenge to improve patient's outcome, and lncRNAs are involved in the carcinogenesis and progression of NSCLC. Accordingly, this study was aimed to explore the roles and functions of lncRNA FENDRR in the progression and drug resistance of NSCLC. Methods: The University of California Santa Cruz (UCSC) Xena browser was used to validate the putative profile of lncRNA FENDRR in pan-cancer tissues, whereas Kaplan-Meier analysis was conducted to assess the overall survival rate. The potential mechanism underlying cisplatin (DDP) resistance was then investigated using transfection of siRNA-FENDRR or pcDNA3.1/FENDRR *in vitro* and *in vivo*. Simultaneously, subcellular localization of FENDRR, along with targeted DiGeorge syndrome critical region 8 (DGCR8), was predicted using lncATLAS database and further ascertained by RNA immunoprecipitation, fluorescence *in situ* hybridization and western blotting. Results: LncRNA FENDRR was lowly expressed in 28 types of tumor tissues, especially in A549/DDP-resistant cells and the patients with DDP resistance. LncRNA FENDRR downregulation was associated with poor survival for patients with NSCLC. Conversely, FENDRR overexpression was observed to suppress cell viability and clonogenic ability, enhance sensitivity to cisplatin in DDP-resistant NSCLC cells and simultaneously induced their apoptosis. However, FENDRR knockdown led to opposite effects on A549 cells. Furthermore, FENDRR was predominantly located in nucleus, where its overexpression suppressed tumor proliferation in A549/DDP cells by directly targeting DGCR8. Conclusions: Taken together, these findings suggest evidence of FENDRR in the emergence of NSCLC and further reveal a key role of the FENDRR/DGCR8 axis in the progression and drug resistance in this cancer, thereby implicating a FENDRR-targeted therapeutic strategy for combating DDP resistance in NSCLC.

Keywords: Long noncoding RNA, forkhead box (FOX) F1 adjacent non-coding developmental regulatory RNA, non-small cell lung cancer, cell proliferation, DiGeorge syndrome critical region 8

Introduction

Lung cancer is one of the primary contributors to cancer-related mortality across the world, with the highest mortality rates for both men and women. In clinical settings, lung cancer mainly presents as two major histological subtypes, namely small cell lung carcinoma (SCLC) and non-SCLC (NSCLC), where the latter constitutes 80-85% of all cases [1, 2]. In 2025, there were 226,650 newly diagnosed patients with lung and bronchial cancer (110,680 males and 115,970 females) in the United States, with estimated deaths of 124,730 (64,190 males and 60,540 females) for these diseases [3]. Despite great recent advancements in the field of NSCLC diagnosis, the majority of cases are already at an advanced stage at diagnosis, with an overall survival (OS) rate of only 15%. At present, lung cancer continues to be a major public health issue, accounting for 20% of all new cancer cases and ~30% of cases of mortality every year [4]. Notably, it is estimated that the death toll from lung cancer may reach ≥850,000 by 2030 in China [5], which will cause a heavy burden for the country and the society.

Currently, cis-diammine-dichloroplatinum (II) or cisplatin (DDP)-based chemotherapy is the

https://doi.org/10.62347/QKUG5170

foundation of treatment that has been frequently used for patients with NSCLC, especially for those with unresectable NSCLC [6, 7]. Although the latest decade has witnessed advance in therapeutic options for patients with lung cancer, the currently available standard treatment strategy has not yielded significant survival benefits, with a 5-year survival rate of <30% in the majority of countries [8]. Due to distal metastasis and the increasing numbers of recurrences caused by acquired and inherent/intrinsic drug resistance, NSCLC remains to be incurable for the vast majority of cases, posing significant challenges in management of this disease [9, 10]. In terms of drug resistance, it is urgent and necessary to discover novel precise prognostic markers and explore their potential mechanism for improving the survival of patients with NSCLC, especially for those affected by advanced or metastatic cancer.

Long non-coding RNAs (lncRNAs) are defined as RNA transcripts that are >200 nucleotides in length, which have diverse roles in biological pathways. Their mutations and dysregulation may lead to the development and progression of various complex human diseases [11]. Accumulating evidence has identified a vital role of lncRNAs in several types of cancer, including NSCLC [12]. Simultaneously, analyzing large quantities of big data has emphasized lncRNAs as specific diagnostic factors and novel therapeutic targets for NSCLC treatment [13-15]. Various lncRNAs have been reported to be responsible for the development of DDP resistance in lung cancer, such as lncRNA nicotinamide nucleotide transhydrogenase-antisense 1 [16], lncRNA-activated by transforming growth factor beta [17], lncRNA integrin β2-antisense 1 [18], lncRNA alpha-actin 2-antisense 1 (also known as ZXF1) [19], lncRNA small nucleolar RNA host gene 12 [20], and lncRNA RP3-326I13.1 [21]. Accordingly, targeting lncRNAs may serve to be an effective approach for developing novel and promising therapeutics to overcome chemoresistance in lung cancer. DiGeorge syndrome critical region gene 8 (DGCR8), a double-stranded RNA-binding protein, has previously been demonstrated to be a non-catalytic subunit of the microprocessor complex responsible for the regulation of lncRNA stability [22]. Mechanistically, DDP resistance in NSCLC is considered to be a multifactorial process that is mediated in part by enhancing DNA damage repair, activating multidrug efflux, regulating cell cycle progression, increasing resistance to apoptosis, altering signaling pathways and encouraging epithelial-mesenchymal transition [23]. Interestingly, lncRNA forkhead box (FOX) F1 adjacent non-coding developmental regulatory RNA (FENDRR) has been shown to regulate tumor proliferation, migration, and invasion [24]. Abnormal lncRNA FENDRR expression has been found in multiple types of human cancer pathogenesis [25], but its role in the DDP-resistant NSCLC via targeting DGCR8 is scarcely reported.

Based on bioinformatics analysis and clinical correlation analysis, the expression profile of a novel lncRNA FENDRR in NSCLC cells and tissues were screened and validated prior to the evaluation of its expression and role in the prognosis of patients with NSCLC. In addition, transcriptomic and proteomic analysis was applied to reveal a potential critical role of the FENDRR/DGCR8 axis in the progression and drug resistance of NSCLC.

Materials and methods

Bioinformatic analysis

The University of California Santa Cruz (UCSC) Xena browser (https://xenabrowser.net; accessed on 20 June 2024) data were conducted in the initial pan-cancer analysis of FENDRR expression, in addition to the prognosis of patients with NSCLC. Subsequently, Kaplan-Meier analysis was performed to investigate the potential value of FENDRR in the prognosis of patients with NSCLC after application of the following exclusion criteria: i) They had incomplete clinical data; ii) They received surgery; and iii) They had other primary tumors or serious organic disease.

LncATLAS (http://lncatlas.crg.eu/), a web-based visualization tool, was used to verify quantitative information about the subcellular localization of lncRNAs in human NSCLC cells. Furthermore, microRNAs (miRNAs), which may specifically bind with FENDRR, were systematically predicted and ascertained using lncATLAS analysis and CatRAPID omics v2.0 analysis (http://service.tartaglialab.com/page/catrapid_omics2_group), respectively.

Clinical characteristics of patients

From 2022 to 2024, eligible participants planned for regular chemotherapy were recruited in the Department of Thoracic Surgery, Xuzhou Cancer Hospital after diagnosis of NSCLC based on their imaging appearance and histopathological features by two independent pathologists. Exclusion criteria included uncertainty of his/her condition, other concomitant diseases, and being unable to complete assessment. After exclusion criteria, there were 42 males and 38 females in the present study, with a median age of 65.4 years in a range from 27 to 83 years. Meanwhile, 40 paired human samples of primary NSCLC tumor and their matched adjacent paracancerous tissues were initially separated during the surgery and stored in the liquid nitrogen. In addition, DDP-resistant (n=22) and -sensitive (n=18) tumor tissues were collected from patients with NSCLC and frozen to identify whether the FENDRR was differentially expressed in the two groups. All patients were fully informed and signed an informed consent form prior to the study, and all experiments were conducted according to the principles of the Declaration of Helsinki, and the study guidelines were approved by the Ethics Committee of Xuzhou Third People's Hospital Affiliated to Jiangsu University (2024-02-016-K01) in China.

Human cell culture

Bronchial epithelial cell line BEAS-2B and NSCLC cell lines, including A549 (NSCLC; EGFR wild type; CSTR:19375.09.3101HUMSCSP503), HCC827 (NSCLC; EGFR del G746_A750 and TP53 del V218; CSTR:19375.09.3101HUMSCSP538) and NCI-H1264 (lung adenocarcinoma with mutations in *CDKN2A*, *KRAS* and *TP53*; CSTR:16607.09.1101HUM-PUMC000113), were purchased from the Cell Bank of Type Culture Collection of The Chinese Academy of Sciences [26]. Cells were cultured in Roswell Park Memorial Institute (RPMI)-1640 media (Thermo Fisher Scientific, Inc.) with 10% fetal bovine serum (FBS) (Beyotime Institute of Biotechnology) and 1% penicillin/streptomycin (Jiangsu Kaiji Biotechnology Co., Ltd.) at 37°C in an incubator with a humidified atmosphere of 5% CO_2.

Stable DDP-resistant A549 (A549/DDP) cells were purchased from Procell Life Science & Technology Co., Ltd. and cultured in RPMI-1640 media containing a final concentration of 1 μg/ml DDP to maintain DDP resistance. After the cells proliferated to ~80% confluence, experiments were performed.

Plasmid and small interfering RNA (siRNA) transfection

FENDRR and DGCR8 were separately silenced by specific siRNAs, namely si-FENDRR (5'-CUACUAUCUGGACCAUCUA-dTdT-3') and si-DGCR8 (5'-CUGUCAAGUUUGUGCAUAUTT-3'), with scramble siRNAs acting as negative control (siNC) (5'-ACCCAGAGTTCTTTGCTCCGCTTAT-3'). Conversely, FENDRR was overexpressed by transfecting with pcDNA3.1-FENDRR (pcDNA/FENDRR), with empty vector acting as negative control. Following the manufacturer's protocols, the cells with a density of 5×10^5 cells per well were separately cultured in a six-well plate for 24 hours and then incubated with a serum-free transfection complex containing 30 pmol RNA (Guangzhou RiboBio Co., Ltd.) or 2 μg plasmids (Shanghai GenePharma Co., Ltd.) using Lipofectamine 2000 reagent (Invitrogen; Thermo Fisher Scientific, Inc.). Thereafter, transfection efficiency was measured using reverse transcription-quantitative PCR (RT-qPCR). To establish stable clones, the transfected cells were selected with G418 (Invitrogen; Thermo Fisher Scientific, Inc.) for >1 week.

Determination of half maximal inhibitory concentration (IC50) by Cell Counting Kit-8 (CCK-8) assay

According to the manufacture instructions of CCK-8 Assay Kit (Beyotime Institute of Biotechnology), cell viability, along with IC50 of DDP to the transfected or un-transfected A549 and A549/DDP cells, was conducted. Briefly, 100 μl cell medium at a density of 1×10^5 cells/well was cultured in a 96-well culture plate, followed with 0, 2, 4, 6, 8, 10, and 20 μg/ml DDP for 24, 48, 72 and 96 hours. Afterwards, 10 μl CCK-8 working solution was added to each well for another 2-hour incubation, and then the optimal density (OD) was measured at 450 nm on a microplate reader to analyze the toxicity curve of DDP and the IC50 of DDP was calculated with the following the chemical equation. $y=\frac{62}{1+(\frac{x}{0.68})^{5.5}}+10$ for A549 cells and $y'=\frac{63}{1+(\frac{x}{0.85})^{6}}+29$ for A549/DDP cells.

Table 1. The primer sequences of genes

Gene	Forward	Reverse
FENDRR	5'-TAAAATTGCAGATCCTCCG-3'	5'-AACGTTCGCATTGGTTTAGC-3'
DGCR8	5'-GTGCATGCTTGTCCCTTTGG-3'	5'-TGCCAACATACCTCGTAGGG-3'
β-actin	5'-CATGTACGTTGCTATCCAGGC-3'	5'-CTCCTTAATGTCACGCACGA-3'

Colony formation assay

After transfection with indicated siRNA or overexpressing plasmids, the cells were cultured for 36 hours. Subsequently, the transfected cells were cultured in a six-well plate at an initial density of 500 cells/well and incubated with 4 μg/ml DDP for A549 cells and 10 μg/ml DDP for A549/DDP cells in a mixed medium containing 10% FBS, at 37°C in a humidified atmosphere of 5% CO_2 for 14 days. After washing with phosphate buffer solution (PBS), the clones were incubated with 4% paraformaldehyde for 5 minutes and then stained in 0.1% crystal violet solution for 15 minutes, followed by imaging and counting the number of colonies using Image-Pro Plus software (version 6.2; Media Cybernetics, Inc.).

Cell apoptosis by flow cytometry

According to the instructions of Apoptosis and Necrosis Assay kit (Beyotime Institute of Biotechnology), the transfected cells at the density of 1×10^6 cells per well were separately preincubated with 4 μg/ml DDP for A549 cells and 10 μg/ml DDP for A549/DDP cells in 6-well plates for 48 hours. After washing and centrifugation, the cells were placed in 500 μl binding buffer containing 5 μl Annexin V-fluorescein isothiocyanate (FITC) and 10 μl propidium iodide (PI) at room temperature with protection from light for 10 minutes. Subsequently, the apoptotic rate was detected by a FACSCelesta flow cytometry (BD Biosciences, USA) and then the data were analyzed by CellQuest 3.0 software (BD Biosciences).

RNA fluorescence in situ hybridization (FISH)

LncRNA FISH probes were synthesized by Guangzhou RiboBio Co., Ltd. and separately applied to identify the subcellular localization of FENDRR and DGCR8. Briefly, the pre-seeded cells were fixed in the solution of 4% paraformaldehyde for 10 minutes at room temperature and then permeabilized in 0.1% Triton X-100 diluted in PBS (PBST) on ice for 5 minutes. After pre-hybridization for 30 minutes, the cells were incubated with 250 μl hybridization solution containing the probe (300 ng/ml) at 42°C overnight. After rinsing with PBST three times, cell nucleus was stained with 4',6-diamidino-2-phenylindole (DAPI) (1:800, Sigma-Aldrich; Merck KGaA) for 5 minutes, observed and imaged under both BX51 fluorescence microscope (Olympus Corporation) and LSM 710 confocal microscope (Carl Zeiss, AG).

RT-qPCR

According to the instruction of TRIzol reagent solution (Invitrogen; Thermo Fisher Scientific, Inc.) and HiScript II 1st Strand cDNA synthesis kit (Vazyme Biotech Co., Ltd.), total RNA was separated from the pretreated cells and then reversely transcribed into complementary DNA (cDNA). The primer sequences of genes were listed in **Table 1**. qPCR analysis was subsequently performed using ultraSYBR one-step RT-qPCR Kit (CoWin Biosciences). The PCR reaction system and conditions were as follows: 25 ml reaction mixture containing 1× PCR buffer, 0.2 mM dNTPs, 0.2 μM of each primer, 1 unit of Taq DNA polymerase, and 50 ng of template DNA. The thermal cycling conditions consisted of an initial denaturation at 95°C for 5 minutes; followed by 35 cycles of denaturation at 95°C for 30 seconds, annealing at 58°C for 30 seconds, and extension at 72°C for 1 minute; with a final extension at 72°C for 5 minutes. Relative quantification of the mRNA expression of target genes was then performed using the $2^{-\Delta\Delta CT}$ method and normalized to the internal control β-actin according to a previous study [27].

RNA immunoprecipitation (RIP) assay

Following the instructions of the EZ-Magna RIP Kit (cat. no. 17-701, Millipore Sigma), the cells were placed in 4% formaldehyde and then lysed in the RIP lysis buffer. Thereafter, 100 μl cell lysates was incubated with magnetic beads coupled with DGCR8 (cat. no. ab19-1875, Abcam) or Immunoglobulin G (IgG; cat.

no. ab218427, Abcam) to digest remaining co-extracted proteins at 37°C for 2 hours. The immune precipitated RNA was then extracted using TRIzol reagent and subsequently analyzed by RT-qPCR to estimate the interactions between DGCR8 and FENDRR.

Animal study

Twenty-four male BALB/c nude mice (16-18 g; 6-week-old) were purchased from the Comparative Medicine center of Yangzhou University. All mice were housed under 12-h light/dark cycle with a relative humidity of 50±10% at 23-24°C and granted free access *ad libitum* to standard rodent chow and tap water. To minimize pain and injury, all animal study procedures complied strictly with the Animal Research Guidelines and they were approved by the Institutional Animal Guidelines of Xuzhou Third People's Hospital Affiliated to Jiangsu University (202409T010). A549 cells transfected with si-FENDRR (or si-NC) and A549/DDP cells transfected with FENDRR (or vector), at a density of 1.5×10^6 cells/100 μl/per mouse, were subcutaneously inoculated into the right flank area of the mice to develop FENDRR-knockdown A549 cell xenograft-bearing nude mice, FENDRR-overexpressing A549/DDP-cell xenograft-bearing nude mice, and their corresponding controls (n=6 in each group), respectively. Throughout the experimental period, body weight and tumor size were assessed every 5 days and the tumor volume (TV) was calculated using the following formula: TV (mm^3) = length × $(width)^2/2$. Once the tumor volume was >1,000 mm^3 or approximately equivalent to a tumor with a diameter of 17 mm in a 25 g mouse during the experiment or at the end of the experimental animal study, each mouse was intraperitoneally injected a euthanizing dose (200 mg/kg) of sodium pentobarbital (Sigma-Aldrich Inc., USA). All tumors were accurately removed, weighted and photographed. Thereafter, the tumor tissues were dissected for histological analysis.

Immunohistochemical (IHC) analysis

Ki-67 is a key molecular marker used to indicate the proliferative activity of tumor cells [28]. Therefore, its expression in tumor tissues was detected by IHC analysis. Briefly, tumor tissues were collected, fixed overnight with 10% formaldehyde, dehydrated, embedded in paraffin and then cut into sections of 4-μm thickness. After heating in antigen retrieval buffer for 2 minutes and blockading the endogenous peroxidase activity in the solution of 3% hydrogen peroxide for 12 minutes, the tissue sections were blocked for 30 minutes in 2% bovine serum albumin (BSA) (w/v) (cat. no. ST025; Beyotime Institute of Biotechnology). Subsequently, they were incubated with an anti-Ki-67 antibody (1:200, cat. no. ab19754, Abcam) overnight at 4°C and then with the same genus secondary antibody (1:500, cat. no. ab150117, Abcam) for 1 hour at room temperature. After rinsing with PBS three times for 5 minutes each, the tumor sections were visualized, with any detectable nuclear staining (dotted or diffuse) as a positive threshold. Based on the percentage of positively stained cells and their staining intensity, the expression of Ki-67 was scored in duplicate by two experienced pathologists under a BX51 fluorescence microscope (Olympus Corporation).

Western blotting analysis

After treatment for 24 hours, the transfected A549 and A549/DDP cells were separately harvested and suspended in radioimmunoprecipitation assay buffer (cat. no. P0039, Beyotime Institute of Biotechnology) containing the protease inhibitor phenylmethane sulfonyl fluoride for extraction of total cellular protein. After centrifugation, the supernatants were collected for quantifying the protein concentration using a Bicinchoninic Acid Protein Assay Kit (cat. no. C05-02001, Bioss, China). The denatured proteins were then separated by 10% sodium dodecyl sulfate-polyacrylamide gel electrophoresis and subsequently electroblotted onto polyvinylidene fluoride membranes. After blocking non-specific binding sites in PBS supplemented with 5% BSA (cat. no. ST025, Beyotime Institute of Biotechnology) for 2 hours at room temperature, the membranes were incubated with diluted specific primary antibody against DGCR8 (1:1,000, cat. no. ab191875, Abcam) at 4°C. The following day, the unbound primary antibody was washed out with 1× TBST solution and then the blots were incubated with a horseradish peroxidase-conjugated secondary antibody (1:3,000, cat. no. ab6759, Abcam) for 60 minutes at room temperature. After washing again, the bands were visualized using an Enhanced Chemiluminescence Kit (Amersham;

Cytiva) and the gray value was then analyzed with ImageJ 1.51 software (National Institutes of Health), with the western protein marker (cat. no. G2091, Wuhan Servicebio Technology Co., Ltd.) used for molecular weight estimation. In addition, β-actin (1:5,000, cat. no. ab8227, Abcam) served as the internal control for the quantitative analysis of protein.

Statistical analysis

Statistical analyses were determined using SPSS v26.0 (IBM Corp.). All data were recorded as mean ± standard deviation and a comparison between the two groups was conducted using two-tailed Student's independent samples or paired samples t-test as appropriate. The Kaplan-Meier method was used to analyze FENDRR on overall survival of patients. P<0.05 was considered to indicate a statistically significant difference.

Results

Expression of LncRNA FENDRR in pan-cancer tissues and its association with OS in patients with NSCLC

Based on the UCSC Xena browser data, RNA-seq data of 34 types of cancers were acquired from the Cancer Genome Atlas database, Target database, and Genotype-Tissue Expression database. Compared with the corresponding adjacent paracancerous tissues, FENDRR expression was significantly lower (*P*<0.05) in 28 tumor tissues, including lung adenocarcinoma (n=513) and lung squamous cell carcinoma (n=498), but not in pan-kidney cohort, head and neck squamous cell carcinoma and cholangiocarcinoma tissues. In addition, compared with the corresponding adjacent paracancerous tissues, the unpaired samples t-test showed a high expression of FENDRR in both kidney renal clear cell carcinoma and pancreatic adenocarcinoma (P<0.05), but not in the pheochromocytoma and paraganglioma (**Figure 1A**).

After application of the exclusion criteria, 457 cases of NSCLC were involved in the present study and they were separated into high- and low-FENDRR subgroups according to its median expression level. Afterwards, Kaplan-Meier analysis of patients with NSCLC demonstrated that low expression of FENDRR (n=230) was associated with worse OS (P<0.01), but there were no significant differences between the two subgroups after initial diagnosis for 1,812, 3,624, 5,436 and 7,248 days (**Figure 1B**).

To verify the reliability and accuracy of RNA-seq data analysis, RT-qPCR was conducted to validate the expression of FENDRR in 40 cases of lung cancer tissues and their matched adjacent paracancerous tissues from the present hospital. Compared with the corresponding paracancerous tissues, the paired samples t-test showed a lower expression level of FENDRR in the lung cancer tissues (P<0.05, **Figure 2A**). Conversely, the unpaired samples t-test analysis of tissue samples from patients with NSCLC further revealed a lower expression level of FENDRR in the DDP-resistant group compared with the DDP-sensitive group (P<0.05, **Figure 2B**).

To further ascertain the roles of FENDRR in the occurrence and progress of NSCLC, its expression level was next determined in a variety of NSCLC cell lines. Compared with human BEAS-2B cells, the level of FENDRR expression was observed to be significantly decreased in the NSCLC cell lines, including A549, HCC827 and H1264 (P<0.05, **Figure 2C**), especially in the A549/DDP cells (**Figure 2D**). A549/DDP cells along with parental A549 cells were therefore selected for subsequent experimental studies. Kaplan-Meier analysis of patients with different levels of FENDRR expression showed that OS rate was significantly lower in the low expression of FENDRR group than that in the high expression of FENDRR group (P=0.01762, HR= 0.62, 95% CI: 0.45-0.85, **Figure 2E**). Cell viability was suppressed in a dose-dependent manner in NSCLC cells, where the IC50 value of DDP was higher in A549/DDP cells than that in A549 cells (7.39 μg/ml vs. 3.18 μg/ml; P<0.05, **Figure 2F**). These findings suggest that FENDRR may be implicated in the oncogenesis and chemotherapy resistance in NSCLC.

Expression profiles of lncRNA FENDRR in NSCLC cells and it's in vitro effects on cell proliferation, clone formation and cell apoptosis

After transfection with si-FENDRR or pcDNA3.1/FENDRR for 24 hours, RT-qPCR analysis validated that the relative expression of FENDRR was significantly downregulated in the si-FENDRR group compared with the si-NC group (P<0.05, **Figure 3A**). By contrast, the relative expression of FENDRR in A549/DDP cells was

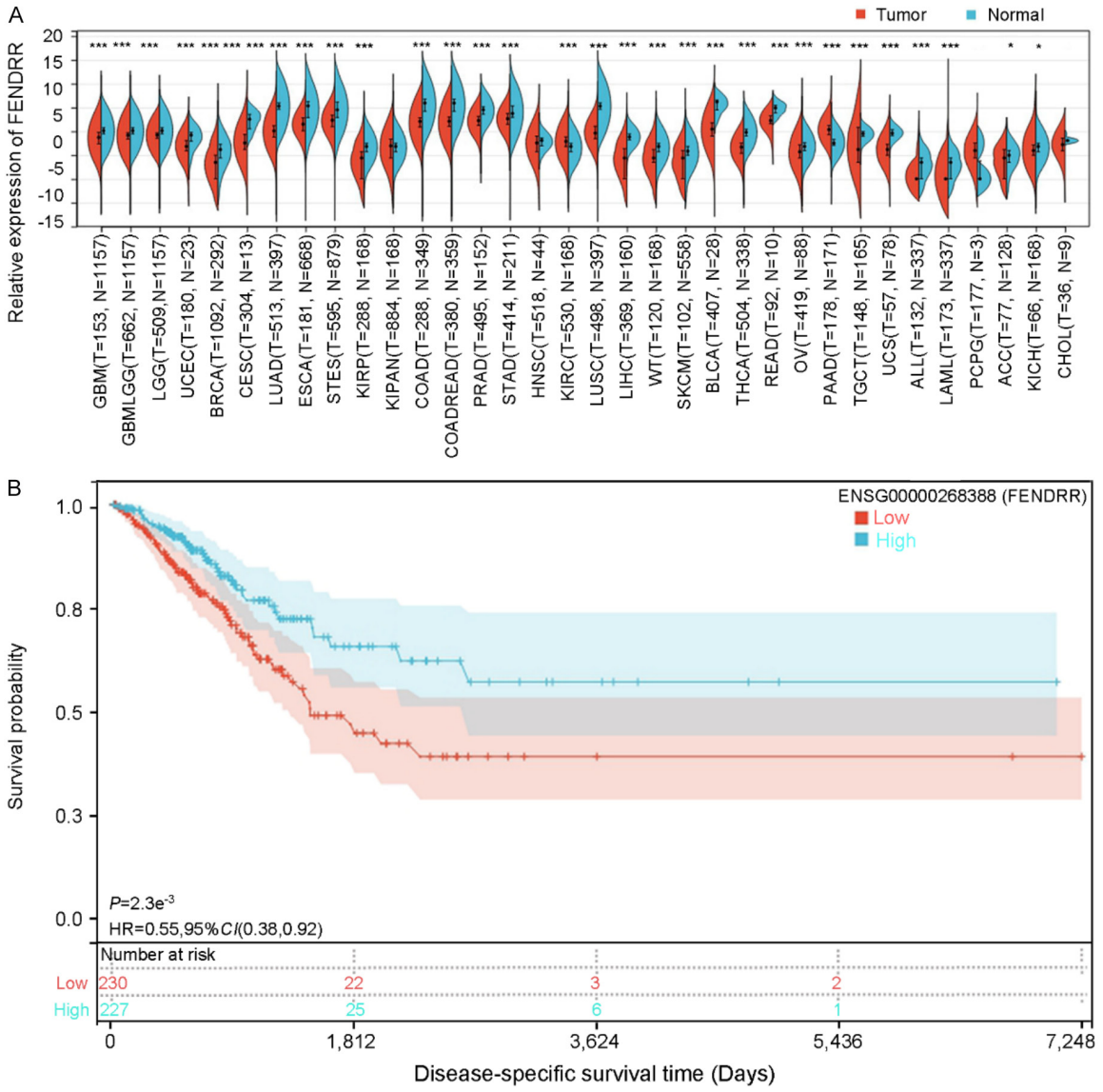

Figure 1. Relative expression of FENDRR and its clinical significance. A. Relative expression of FENDRR in pan-cancer tissues and matched adjacent paracancerous tissues. B. Clinical significance of FENDRR in the survival of NSCLC patients. *; P<0.05, ***; P<0.001, compared with matched adjacent paracancerous tissues. ACC, adrenocortical carcinoma; ALL, acute lymphoblastic leukemia; BLCA, bladder urothelial carcinoma; BRCA, breast invasive carcinoma; CESC, cervical squamous cell carcinoma; CI, confidence interval; COAD, colon adenocarcinoma; COADREAD, colon adenocarcinoma/rectum adenocarcinoma esophageal carcinoma; CHOL, cholangiocarcinoma; ESCA, esophageal carcinomas; FENDRR, forkhead box (FOX) F1 adjacent noncoding developmental regulatory RNA; HR, hazard ratio; GBM, glioblastoma multiforme; GBMLGG, glioma; HNSC, head and neck squamous cell carcinoma; KICH, kidney chromophobe; KIPAN, pan-kidney cohort (KICH+KIRC+KIRP); KIRP, kidney renal papillary cell carcinoma; KIRC, kidney renal clear cell carcinoma; LAML, acute myeloid leukemia; LGG, brain lower grade glioma; LIHC, liver hepatocellular carcinoma; LUAD, lung adenocarcinoma; LUSC, lung squamous cell carcinoma; OV, ovarian serous cystadenocarcinoma; PAAD, pancreatic adenocarcinoma; PCPG, pheochromocytoma and paraganglioma; PRAD, prostate adenocarcinoma; READ, rectum adenocarcinoma; SKCM, skin cutaneous melanoma; STAD, stomach adenocarcinoma; STES, stomach and esophageal carcinoma; TGCT, testicular germ cell tumors; THCA, thyroid carcinoma; UCEC, uterine corpus endometrial carcinoma; UCS, uterine carcinosarcoma; WT, wilms.

significantly overexpressed in the FENDRR group compared with the vector control group (P<0.05, **Figure 3B**). After transient transfection and repeated culture, CCK-8 assay revealed that both cell viability and IC50 value of A549 cells were significantly higher in the si-FENDRR group than those in the si-NC group (P<0.05, **Figure 3C**). Conversely, cell prolifera-

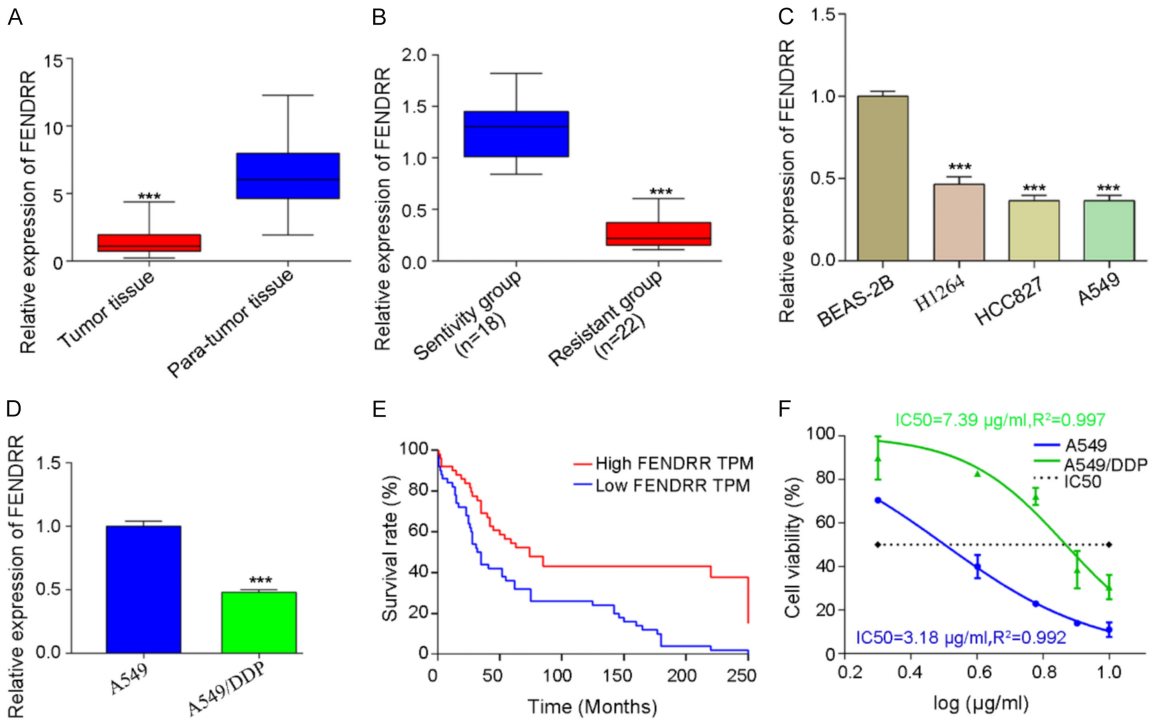

Figure 2. Confirmation of FENDRR expression and its effect on the cell viability and survival rate of NSCLC patients. A. Tumor tissues and para-tumor tissues. B. Cisplatin-resistant and -sensitive patients with NSCLC. C. Lung cancer cell lines and BEAS-2B cells. D. Cisplatin-resistant and -sensitive NSCLC cells. E. Overall survival (OS) of NSCLC patients. F. Cell viabilities and half maximal inhibitory concentration (IC50) value of cisplatin in A549/DDP cells and parental A549 cells. ***; P<0.001, compared with control group.

tion was suppressed whereas the IC50 value of A549/DDP cells deceased significantly in the FENDRR group compared with the vector control group (P<0.05, **Figure 3D**). Therefore, it could be inferred that low expression of FENDRR can be clinically used to predict ineffective response to DDP-associated chemotherapy.

The clonogenic potential role of FENDRR was next investigated using colony formation assay. After transfection with si-FENDRR or pcDNA3.1/FENDRR for 24 hours and subsequent crystal violet staining, the number of colonies increased significantly in A549 cells (**Figure 3E**), whereas it decreased markedly in A549/DDP cells (**Figure 3F**) compared with corresponding controls. Similarly, flow cytometric analysis found that the apoptotic rate decreased markedly in the si-FENDRR transfected A549 cells (**Figure 3G**), whilst it increased significantly in the pcDNA3.1/FENDRR transfected A549/DDP cells (**Figure 3H**). In summary, overexpression of FENDRR was suggested to suppress cell proliferation and clonogenic ability, decrease the IC50 value of DDP and induce apoptosis in A549/DDP cells. By contrast, FENDRR knockdown may lead to the opposite effects on A549 cells, implying that overexpression of FENDRR sensitizes DDP-resistant NSCLC cells to DDP.

In vivo antitumor effects of lncRNA FENDRR overexpression via enhancing the sensitivity of cisplatin

After 20 day-inoculation, both tumor volume and tumor weight were found to be significantly larger in the FENDRR-knockdown A549 cell xenograft-bearing nude mice compared with the si-NCs (P<0.05). Notably, the enhanced tumor suppression was observed in the FENDRR-overexpressing A549/DDP-cell xenograft-bearing nude mice compared with the vector controls (*P*<0.05, **Figure 4A-D**).

IHC analysis showed that the expression level of Ki-67 protein increased significantly in the FENDRR-knockdown A549 cell xenograft-bearing nude mice compared with the si-NCs. By contrast, the expression level of Ki-67 protein decreased markedly in the FENDRR-overexpressing A549/DDP cell xenograft-bearing nude mice compared with the vector controls

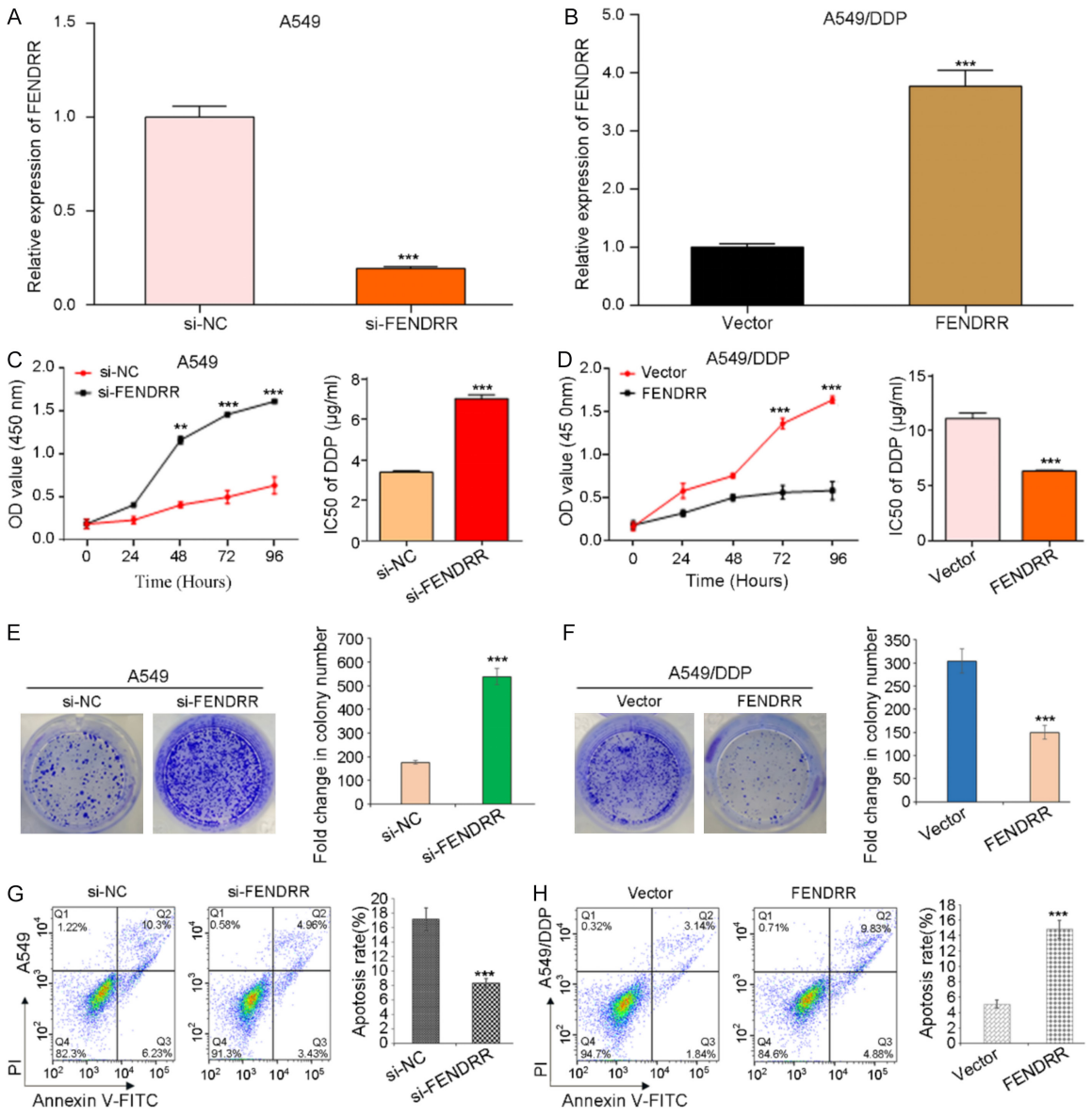

Figure 3. Transfection efficiency of lncRNA FENDRR and its effect on cell proliferation, clone formation, and cell apoptosis after separately transfection with si-FENDRR and pcDNA3.1/FENDRR. A. Validation of FENDRR expression in FENDRR-knockdown A549 cells. B. Validation of FENDRR expression in FENDRR-overexpressing A549/DDP cells. C. Cell viability and half maximal inhibitory concentration (IC50) in FENDRR-knockdown A549 cells. D. Cell viability and IC50 value of FENDRR-overexpressing A549/DDP cells. E. Representative image of colony formation and clone formation rates in the FENDRR-knockdown A549 cells. F. Representative image of colony formation and clone formation rates in the FENDRR-overexpressing A549/DDP cells. G. Representative flow cytometry images of cell apoptosis and apoptosis rates in the FENDRR-knockdown A549 cells. H. Representative flow cytometry images of cell apoptosis and apoptosis rates in the FENDRR-overexpressing A549/DDP cells. Q1, Q2, Q3 and Q4 separately indicate debris cell population, late apoptotic cell population, early apoptotic cell population, and healthy cell population. Finally, apoptotic rate (%) = percentage of (Q2+Q3) (n=3). **P<0.01, ***P<0.001, compared with control group. OD, optical density; FITC, fluorescein isothiocyanate; PI, propidium iodide.

(**Figure 4E**). These data indicate that the overexpression of FENDRR can suppress tumor proliferation in DDP-resistant NSCLC, whereas FENDRR knockdown can promote tumor proliferation in the DDP-sensitive NSCLC *in vivo*.

Subcellular localization of lncRNA FENDRR and identification of its directed target gene

To investigate how lncRNA FENDRR functions in NSCLC, candidate proteins associated with

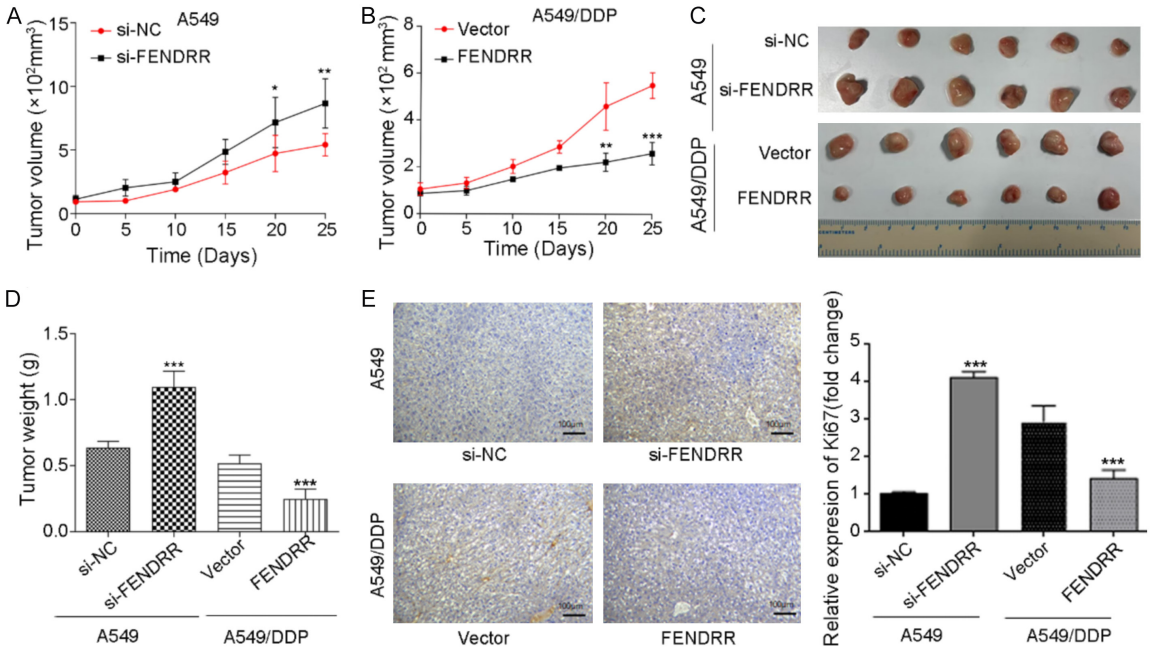

Figure 4. Effect of lncRNA FENDRR on the tumor growth in tumor-bearing mice. A, B. Tumor growth curve in the FENDRR-knockdown A549-cell xenograft-bearing nude mice and FENDRR-overexpressing A549/DDP-cell xenograft-bearing nude mice. C. Representative images of the resected tumors in both FENDRR-knockdown A549-cell xenograft-bearing nude mice (upper) and FENDRR-overexpressing A549/DDP-cell xenograft-bearing nude mice (lower). D. Tumor weight in both FENDRR-knockdown A549-cell xenograft-bearing nude mice (left) and FENDRR-overexpressing A549/DDP-cell xenograft-bearing nude mice (right). E. Representative images and relative expression of Ki-67 protein in the FENDRR-knockdown A549-cell xenograft-bearing nude mice (upper) and FENDRR-overexpressing A549/DDP-cell xenograft-bearing nude mice (lower) (Magnification: 100×). *; P<0.05, **; P<0.01, ***; P<0.001, compared with control group.

FENDRR were next predicted and identified. LncATLAS analysis of pan-cancer cells suggested a similar cytoplasmic-to-nuclear relative concentration index (CNRCI) of A549 cells and it was 0.1 PFKM (**Figure 5A**), referring to the control of HOX transcript antisense RNA (HOTAIR) [29]. Then, CatRAPID omics v2.0 analysis ascertained that FENDRR (5'-UUAGGGAUUC-CCC-UCCAAGG-3') had an ability to specifically bind to DGCR8 (3'-AAUCCAUAG--GGGAGGUUCU-5') (**Figure 5B**). Consistently, RIP assay further confirmed that FENDRR could directly interact with DGCR8 (**Figure 5C**).

To further examine the subcellular distribution of the two proteins, RNA-FISH and fluorescent microscope images of cells were performed. The overall distribution of FENDRR was found to be similar to that of DAPI staining except for a relative weak fluorescence intensity of FENDRR, implying a co-localization of FENDRR with DAPI in the nuclei of A549 cells and a relative low expression of FENDRR (**Figure 5D**). Similarly, both FENDRR and DGCR8 were observed to be distributed in the nuclei except for the relative weak fluorescence intensity of FENDRR under a confocal microscope (**Figure 5E**). Furthermore, western blotting confirmed that FENDRR knockdown suppressed the expression of DGCR8 in A549 cells (**Figure 5F**), whereas overexpression of FENDRR promoted the expression of DGCR8 in A549/DDP cells (**Figure 5G**). Collectively, these data indicate that FENDRR may directly bind to the double-stranded RNA-binding protein DGCR8.

Reversal of the lncRNA FENDRR-modulated DDP resistance of NSCLC through DGCR8 knockdown

To further validate the role of DGCR8 in the FENDRR-modulated DDP resistance of NSCLC, the transcription and protein expression levels of DGCR8 were separately determined by RT-qPCR and western blotting. As expected in A549/DDP cells, the transcription of DGCR8 (**Figure 6A**) and expression level of DGCR8 protein (**Figure 6B**) were downregulated in the si-

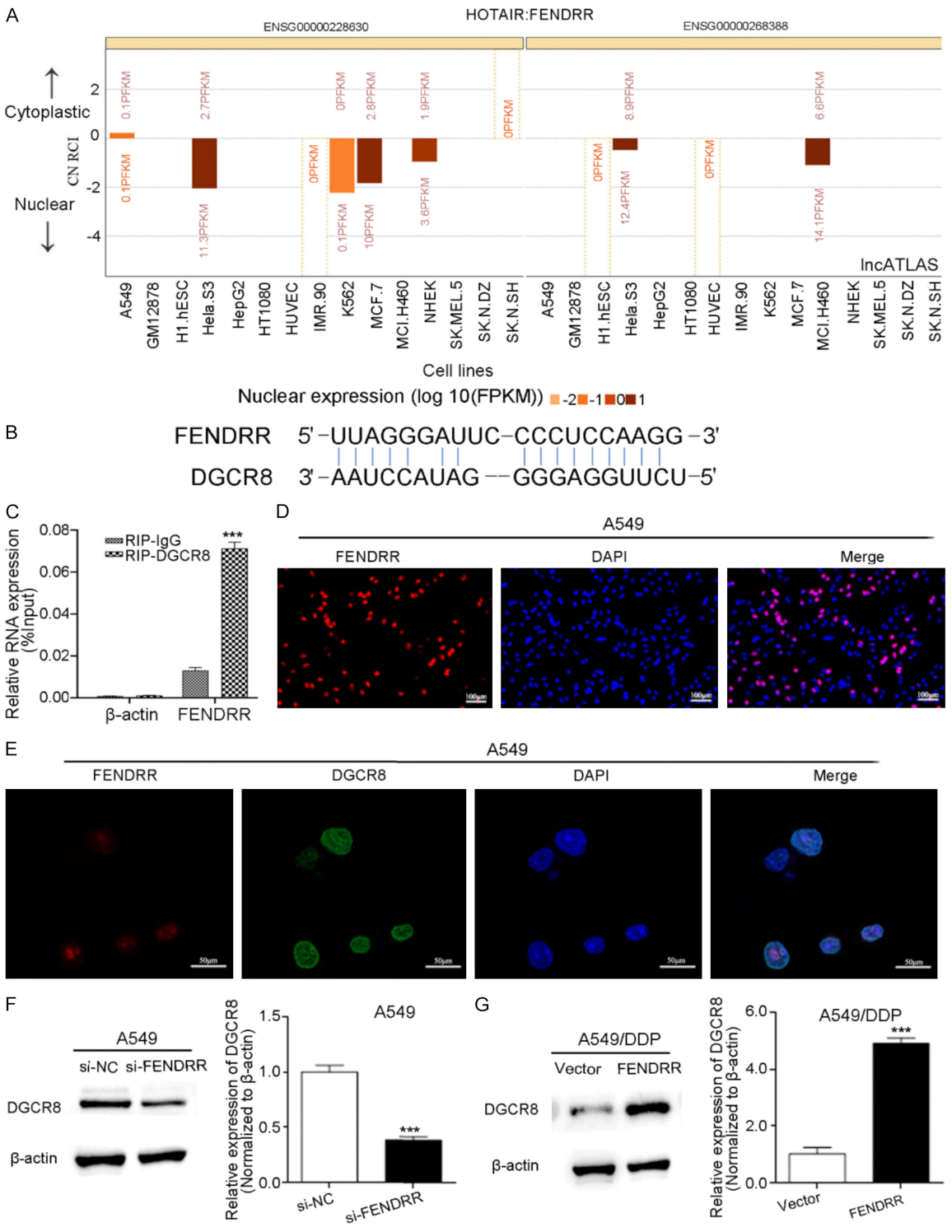

Figure 5. Subcellular localization of lncRNA FENDRR and identification of its direct target gene in NSCLC. A. Subcellular localization plots of FENDRR predicted by LncATLAS in reference to HOTAIR, and bars representing CN-RCI values for the selected genes across cell lines. B. Base complementarity between FENDRR and DGCR8. C. Relative expression of DGCR8 in A549 cells by RIP assay. D. Ascertaining subcellular localization of FENDRR and DGCR8 by FISH assay (Bar: 100 μm; magnification: 100×). E. Ascertaining subcellular localization of FENDRR and DGCR8 under confocal microscope (Bar: 50 μm; magnification: 640×). F. Representative blots and relative expression levels of DGCR8 protein in A549 cells. G. Representative blots and relative expression levels of DGCR8 protein in A549/DDP cells. ***; P<0.001, compared with control group. RIP, RNA immunoprecipitation; CNRCI, cytoplasmic-to-nuclear relative concentration index.

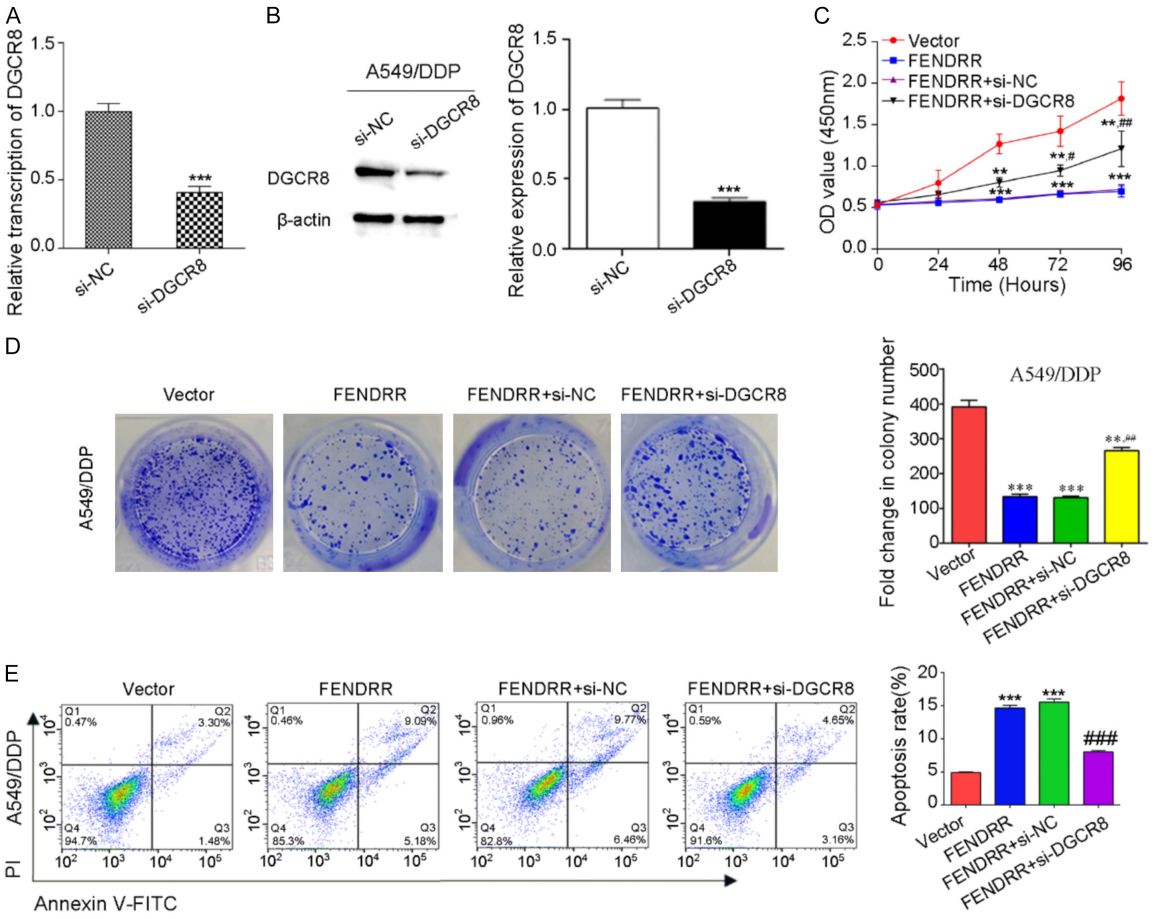

Figure 6. Relative expression of DGCR8 and its effect on the cell proliferation, clone formation, and cell apoptosis in A549/DDP transfected with or without si-DGCR8. A. Validation of DGCR8 transcription level. B. Representative blots and relative expression levels of DGCR8 protein. C. Effect of FENDRR on cell viabilities. D. Representative images of colony formation and clone formation rates. E. Representative images of flow cytometric apoptosis and quantitative analysis of apoptosis rate. Q1, Q2, Q3 and Q4 separately indicate debris cell population, late apoptotic cell population, healthy cell population, and early apoptotic cell population (n=3). Finally, Apoptotic rate (%) = percentage of (Q2+Q3). **; P<0.01, ***; P<0.001, compared with vector group; ##; P<0.01, ###; P<0.001, compared with FENDRR+si-NC group. FITC, fluorescein isothiocyanate; PI, propidium iodide.

DGCR8 group compared with control group. Overexpression of FENDRR led to a significant increase in cell proliferation and clone formation rates, accompanied with a marked decrease in cell apoptosis (**Figure 6C-E**) in the transfected A549/DDP cells. Notably, the aforementioned effects of FENDRR overexpression could be reversed by DGCR8 knockdown (**Figure 6C-E**), revealing that the FENDRR/DGCR8 axis can contribute to DDP resistance in NSCLC.

Discussion

Although the existing data concerning expression profiling of lncRNAs in lung cancer are substantial, it is unclear whether there are associations of lncRNA FENDRR expression with the progression and drug resistance of NSCLC [30]. Low expression of FENDRR was detected in a wide range of human cancers, including NSCLC, especially in the DDP-resistant patients with NSCLC, whereas its downregulation was associated with an unfavorable prognosis. By contrast, *in vitro* and *in vivo* experiments suggested that overexpression of FENDRR sensitized DDP-resistant NSCLC cells to DDP. To the best of our knowledge, the present study was the first to demonstrate a key role of FENDRR and its partner protein DGCR8 in the progression and drug resistance of NSCLC.

Previous evidence has indicated that lncRNAs are involved in almost all physiological or pathological characteristics, including drug resis-

tance of NSCLC [18, 31, 32]. Based on lncRNA screening and validation by bioinformatics analysis, RT-qPCR and western blotting, lncRNA FENDRR was found to be lowly expressed in several NSCLC cell lines, including A549 [11, 30, 33-36], H1975 [33-35], H1650 [33, 34], HCC827 [33, 34], H1299 [11], H460 [11, 35], H358 [11, 35], PC9 [35], H292 [35], and others (Calu-1, Calu-3, Calu-6, COR-L23, DMS53, H3-58, H2073, HTB-59, HTB-182, LUDLU-1, SK-LU-1 and SK-MES-1) [30]. A similar trend of reduced FENDRR expression was detected in A549, H1264 and HCC827 cells, especially in A549/DDP cells and DDP-resistant NSCLC tissues in the present study. This result was consistent with a previous study documenting a lower expression of FENDRR in A549/DDP cells [36]. Collectively, these results imply that FENDRR depletion is at least in part responsible for the oncogenesis and chemotherapy resistance of NSCLC to DDP.

Downregulation of FENDRR promoted epithelial-mesenchymal transition, stemness and metastasis in NSCLC cells according to a previous study [37]. Clinically, loss of FENDRR function was associated with poor differentiation, advanced pathologies and high TNM stages, accompanied with an unfavorable prognosis of NSCLC [11]. In addition, the expression level of FENDRR was positively associated with both tumor size and tumor differentiation [36]. Notably, patients with high expression of FENDRR had longer OS than those with low expression, according to our present Kaplan-Meier analysis. This finding was similar to a previous study that NSCLC patients with high expression level of FENDRR had a superior outcome to those with low expression (mean survival time, 75.29 months vs. 43.71 months; log-rank P=0.021) [28]. Accordingly, lncRNA FENDRR may be a tumor suppressor in the progression of NSCLC and a promising prognostic factor for NSCLC.

LncRNAs are responsible for the epigenetic activation or silencing of gene expression in the nucleus, where they can participate in the regulation of post-transcriptional gene expression in the cytoplasm [12]. Accordingly, ascertaining nuclear-cytoplasmic localization has become one of the primary sources of evidence when investigating the molecular role of newly discovered lncRNAs. Consistent with a previous study [37], our analysis of lncRNAs and RNA-FISH further revealed a co-localization of FENDRR with DGCR8 in the nucleus of A549 cells, where it executed tumor suppressive effects on NSCLC by binding to its promoters of downstream targets. Further *in vitro* findings found that overexpression of FENDRR inhibited cell proliferation and clonogenic ability, and induced apoptosis of A549/DDP cells with a lower IC50 value of DDP, whereas FENDRR knockdown led to opposite effects on A549 cells. In an *in vitro* functional study of lncRNAs, chemotherapy resistance of A549/DDP cells to DDP was weakened by the overexpression of FENDRR, with a conspicuous depression of IC50, but no further mechanical study was reported [36]. It is worth noting that in A549 cell xenograft-bearing nude mice, FENDRR knockdown promoted tumor growth and higher expression of Ki-67. By contrast, overexpression of FENDRR enhanced tumor suppression in the A549/DDP cell xenograft-bearing nude mice in the present study. These data indicate that the overexpression of FENDRR can restore sensitivity to DDP in DDP-resistant NSCLC cells.

LncRNAs can carry various functions in complex regulatory frameworks in cancers, for which the most probable mechanism of cancer-associated gene regulation was found to be interacted with mRNAs in the lncRNA-miRNA-mRNA network [38]. For instance, FENDRR can regulate doxorubicin-resistance by negatively affecting the posttranscriptional expression of ATP binding cassette subfamily (ABC)B1 and ABCC1 in osteosarcoma cells [39]. Similarly, the functional proto-oncogene FOXC2 and miRNA-4700-3p have been shown to be responsible for the FENDRR-induced multidrug resistance of gastric cancer [40]. On the other hand, DGCR8 knockdown not only inhibited cell proliferation and colony formation but also elevated cell apoptosis in the FENDRR overexpressing A549/DDP cells in the present study. Notably, systemic DGCR8 deletion is lethal due to the early arrested development of proliferation and differentiation in embryonic stem cells [41]. Furthermore, our present mechanistic studies suggested a direct reversal of FENDRR-modulated DDP resistance by binding to DGCR8 in A549/DDP cells. Overall, these data suggest that lncRNA FENDRR is involved in the pathogenesis of NSCLC by regulating target genes, where it can be used as a promising biomarker for the diagnosis and prognosis of NSCLC [15].

To further ascertain the roles and functions of lncRNA FENDRR in the progression and drug resistance of NSCLC, bioinformatic analysis of genomes was conducted. The paired samples of human primary NSCLC and matched adjacent paracancerous tissues, in addition to tumor tissues from DDP-resistant and sensitive patients with NSCLC, were collected to identify the differentially expressed lncRNA FENDRR between the two groups. Although patients who underwent lung cancer surgery were excluded, the exploration of progression and drug resistance of NSCLC may be influenced by the surgically resected cases. Additionally, key findings from bioinformatic analysis were validated using cell lines and cell line-derived xenograft models. Nevertheless, lncRNA FENDRR together with DDP should be further investigated in killing the NSCLC tumor cells, and the precise molecular mechanism targeting the drug resistance should be further explored to improve the survival of patient with NSCLC.

Conclusions

Taken together, the present *in vitro* and *in vivo* findings suggest that lncRNA FENDRR is lowly expressed in NSCLC cells and tissues, especially in the DDP-resistant NSCLC cells and tissues, revealing a possible regulatory network of a FENDRR/DGCR8 axis in tumor progression and DDP resistance in NSCLC cells. Therefore, modulation of FENDRR/DGCR8 may be a therapeutic strategy for combating DDP resistance in NSCLC.

Acknowledgements

This study was supported by the Social Development Projects under the Key Programs of Xuzhou City (KC22097).

Disclosure of conflict of interest

None.

Address correspondence to: Dr. Hao Zhang, Department of Thoracic Surgery, Affiliated Hospital of Xuzhou Medical University, 99 West Huaihai Road, Xuzhou 221006, Jiangsu China. E-mail: haozhang_xz@163.com

References

[1] Hendriks LEL, Remon J, Faivre-Finn C, Garassino MC, Heymach JV, Kerr KM, Tan DSW, Veronesi G and Reck M. Non-small-cell lung cancer. Nat Rev Dis Primers 2024; 10: 71.

[2] Jha SK, De Rubis G, Devkota SR, Zhang Y, Adhikari R, Jha LA, Bhattacharya K, Mehndiratta S, Gupta G, Singh SK, Panth N, Dua K, Hansbro PM and Paudel KR. Cellular senescence in lung cancer: molecular mechanisms and therapeutic interventions. Ageing Res Rev 2024; 97: 102315.

[3] Siegel RL, Kratzer TB, Giaquinto AN, Sung H and Jemal A. Cancer statistics, 2025. CA Cancer J Clin 2025; 75: 10-45.

[4] Wang J, Ying J, Wang Z, Meng X, Wu M and Qian C. Genomic testing and targeted therapy of non-small cell lung cancer in China: a nationwide survey of physicians and clinical pathologists. Ann Palliat Med 2024; 13: 221-229.

[5] Tang W, Liu L, Huang Y, Zhao S, Wang J, Liang M, Jin Y, Zhou L, Liu Y, Tang Y, Xu Z, Zhang K, Tan F, Bi N, Wang Z, Wang F, Li N and Wu N. Opportunistic lung cancer screening with low-dose computed tomography in National Cancer Center of China: the first 14 years' experience. Cancer Med 2024; 13: e6914.

[6] Li C, Fan K, Qu Y, Zhai W, Huang A, Sun X and Xing S. Deregulation of UCA1 expression may be involved in the development of chemoresistance to cisplatin in the treatment of non-small-cell lung cancer via regulating the signaling pathway of microRNA-495/NRF2. J Cell Physiol 2020; 235: 3721-3730.

[7] Cui J, He Y, Zhu F, Gong W, Zuo R, Wang Y, Luo Y, Chen L, Wang C, Huo G, Lu H, Liu Z, Chen P and Guo H. Inetetamab, a novel anti-HER2 monoclonal antibody, exhibits potent synergistic anticancer effects with cisplatin by inducing pyroptosis in lung adenocarcinoma. Int J Biol Sci 2023; 19: 4061-4081.

[8] Barr T, Ma S, Li Z and Yu J. Recent advances and remaining challenges in lung cancer therapy. Chin Med J (Engl) 2024; 137: 533-546.

[9] Donington J, Hu X, Zhang S, Song Y, Arunachalam A, Chirovsky D, Gao C, Lerner A, Jiang A, Signorovitch J and Samkari A. Real-world neoadjuvant treatment patterns and outcomes in resected non-small-cell lung cancer. Clin Lung Cancer 2024; 25: 440-448.

[10] Wu T, Dong Y, Yang X, Mo L and You Y. Crosstalk between lncRNAs and Wnt/β-catenin signaling pathways in lung cancers: from cancer progression to therapeutic response. Noncoding RNA Res 2024; 9: 667-677.

[11] Pan H, Yu T, Sun L, Chai W, Liu X and Yan M. LncRNA FENDRR-mediated tumor suppression and tumor-immune microenvironment changes in non-small cell lung cancer. Transl Cancer Res 2020; 9: 3946-3959.

[12] Yang Q, Wang M, Xu J, Yu D, Li Y, Chen Y, Zhang X, Zhang J, Gu J and Zhang X. LINC02159 promotes non-small cell lung cancer progression via ALYREF/YAP1 signaling. Mol Cancer 2023; 22: 122.
[13] Lu T, Wang Y, Chen D, Liu J and Jiao W. Potential clinical application of lncRNAs in non-small cell lung cancer. Onco Targets Ther 2018; 11: 8045-8052.
[14] Çetinkaya M and Baran Y. MicroRNAs and long non-coding RNAs as novel targets in anticancer drug development. Curr Pharm Biotechnol 2023; 24: 913-925.
[15] Liu Y, Han Y, Zhang Y, Lv T, Peng X and Huang J. LncRNAs has been identified as regulators of Myeloid-derived suppressor cells in lung cancer. Front Immunol 2023; 14: 1067520.
[16] Wang H, Guo M, Ding D, Yang F and Chen Z. Long non-coding RNA NNT-AS1 contributes to cisplatin resistance via miR-1236-3p/ATG7 axis in lung cancer cells. Onco Targets Ther 2020; 13: 3641-3652.
[17] Fu N, Niu X, Wang Y, Du H, Wang B, Du J, Li Y, Wang R, Zhang Y, Zhao S, Sun D, Qiao L and Nan Y. Role of LncRNA-activated by transforming growth factor beta in the progression of hepatitis C virus-related liver fibrosis. Discov Med 2016; 22: 29-42.
[18] Chen H, Wang L, Liu J, Wan Z, Zhou L, Liao H and Wan R. LncRNA ITGB2-AS1 promotes cisplatin resistance of non-small cell lung cancer by inhibiting ferroptosis via activating the FOSL2/NAMPT axis. Cancer Biol Ther 2023; 24: 2223377.
[19] Yu T, Bai W, Su Y, Wang Y, Wang M and Ling C. Enhanced expression of lncRNA ZXF1 promotes cisplatin resistance in lung cancer cell via MAPK axis. Exp Mol Pathol 2020; 116: 104484.
[20] Tan D, Wang S, Zhang P, Peng C and Wu T. LncRNA SNHG12 decreases non-small cell lung cancer cell sensitivity to cisplatin by repressing miR-525-5p and promoting XIAP. Ann Clin Lab Sci 2023; 53: 64-75.
[21] Zhou H, Huang X, Shi W, Xu S, Chen J, Huang K and Wang Y. LncRNA RP3-326I13.1 promotes cisplatin resistance in lung adenocarcinoma by binding to HSP90B and upregulating MMP13. Cell Cycle 2022; 21: 1391-1405.
[22] Zhang F, Ruan X, Ma J, Liu X, Zheng J, Liu Y, Liu L, Shen S, Shao L, Wang D, Yang C, Cai H, Li Z, Feng Z and Xue Y. DGCR8/ZFAT-AS1 promotes CDX2 transcription in a PRC2 complex-dependent manner to facilitate the malignant biological behavior of glioma cells. Mol Ther 2020; 28: 613-630.
[23] Saadh MJ, Rasulova I, Almoyad MAA, Kiasari BA, Ali RT, Rasheed T, Faisal A, Hussain F, Jawad MJ, Hani T, Sârbu I, Lakshmaiya N and Ciongradi CI. Recent progress and the emerging role of lncRNAs in cancer drug resistance; focusing on signaling pathways. Pathol Res Pract 2024; 253: 154999.
[24] Zhao X, Wu J, Li Y, Ye F and Wang C. Long noncoding RNA FENDRR inhibits the stemenss of colorectal cancer cells through directly binding to Sox2 RNA. Bioengineered 2021; 12: 8698-8708.
[25] Qian G, Jin X and Zhang L. LncRNA FENDRR upregulation promotes hepatic carcinoma cells apoptosis by targeting miR-362-5p via NPR3 and p38-MAPK pathway. Cancer Biother Radiopharm 2020; 35: 629-639.
[26] Xia M, Zhu W, Tao C, Lu Y and Gao F. LncRNA LASTR promote lung cancer progression through the miR-137/TGFA/PI3K/AKT axis through integration analysis. J Cancer 2022; 13: 1086-1096.
[27] Livak KJ and Schmittgen TD. Analysis of relative gene expression data using real-time quantitative PCR and the 2(-Delta Delta C(T)) Method. Methods 2001; 25: 402-408.
[28] Li Z, Li F, Pan C, He Z, Pan X, Zhu Q, Wu W and Chen L. Tumor cell proliferation (Ki-67) expression and its prognostic significance in histological subtypes of lung adenocarcinoma. Lung Cancer 2021; 154: 69-75.
[29] Kufukihara R, Tanaka N, Takamatsu K, Niwa N, Fukumoto K, Yasumizu Y, Takeda T, Matsumoto K, Morita S, Kosaka T, Aimono E, Nishihara H, Mizuno R and Oya M. Hybridisation chain reaction-based visualisation and screening for lncRNA profiles in clear-cell renal-cell carcinoma. Br J Cancer 2022; 127: 1133-1141.
[30] Acha-Sagredo A, Uko B, Pantazi P, Bediaga NG, Moschandrea C, Rainbow L, Marcus MW, Davies MPA, Field JK and Liloglou T. Long non-coding RNA dysregulation is a frequent event in non-small cell lung carcinoma pathogenesis. Br J Cancer 2020; 122: 1050-1058.
[31] Shen Q, Zhou H, Zhang M, Wu R, Wang L, Wang Y and Chen J. Super enhancer-LncRNA SENCR promoted cisplatin resistance and growth of NSCLC through upregulating FLI1. J Clin Lab Anal 2022; 36: e24460.
[32] Ge P, Cao L, Zheng M, Yao Y, Wang W and Chen X. LncRNA SNHG1 contributes to the cisplatin resistance and progression of NSCLC via miR-330-5p/DCLK1 axis. Exp Mol Pathol 2021; 120: 104633.
[33] Zhang G, Wang Q, Zhang X, Ding Z and Liu R. LncRNA FENDRR suppresses the progression of NSCLC via regulating miR-761/TIMP2 axis. Biomed Pharmacother 2019; 118: 109309.
[34] Zhang MY, Zhang ZL, Cui HX, Wang RK and Fu L. Long non-coding RNA FENDRR inhibits NSCLC cell growth and aggressiveness by sponging miR-761. Eur Rev Med Pharmacol Sci 2018; 22: 8324-8332.

[35] Gong F, Dong D, Zhang T and Xu W. Long non-coding RNA FENDRR attenuates the stemness of non-small cell lung cancer cells via decreasing multidrug resistance gene 1 (MDR1) expression through competitively binding with RNA binding protein HuR. Eur J Pharmacol 2019; 853: 345-352.

[36] Xu R and Han Y. Long non-coding RNA FOXF1 adjacent non-coding developmental regulatory RNA inhibits growth and chemotherapy resistance in non-small cell lung cancer. Arch Med Sci 2019; 15: 1539-1546.

[37] Miao L, Huang Z, Zengli Z, Li H, Chen Q, Yao C, Cai H, Xiao Y, Xia H and Wang Y. Loss of long noncoding RNA FOXF1-AS1 regulates epithelial-mesenchymal transition, stemness and metastasis of non-small cell lung cancer cells. Oncotarget 2016; 7: 68339-68349.

[38] Braga EA, Fridman MV, Burdennyy AM, Loginov VI, Dmitriev AA, Pronina IV and Morozov SG. Various lncRNA mechanisms in gene regulation involving miRNAs or RNA-binding proteins in non-small-cell lung cancer: main signaling pathways and networks. Int J Mol Sci 2023; 24: 13617.

[39] Kun-Peng Z, Xiao-Long M and Chun-Lin Z. LncRNA FENDRR sensitizes doxorubicin-resistance of osteosarcoma cells through down-regulating ABCB1 and ABCC1. Oncotarget 2017; 8: 71881-71893.

[40] Liu H, Zhang Z, Han Y, Fan A, Liu H, Zhang X, Liu Y, Zhang R, Liu W, Lu Y, Fan D, Zhao X and Nie Y. The FENDRR/FOXC2 axis contributes to multidrug resistance in gastric cancer and correlates with poor prognosis. Front Oncol 2021; 11: 634579.

[41] Wang Y, Medvid R, Melton C, Jaenisch R and Blelloch R DGCR8 is essential for microRNA biogenesis and silencing of embryonic stem cell self-renewal. Nat Genet 2007; 39: 380-385.